Available online at www.sciencedirect.com
SCIENCE DIRECT
Journal of Chromatography A, 1094 (2005) 105–117
JOURNAL OF CHROMATOGRAPHY A
www.elsevier.com/locate/chroma

Characterization of a gel-separated unknown glycoprotein by liquid chromatography/multistage tandem mass spectrometry Analysis of rat brain Thy-1 separated by sodium dodecyl sulfate-polyacrylamide gel electrophoresis

Satsuki Itoh [a], Nana Kawasaki [a,b,*], Akira Harazono [a], Noritaka Hashii [a], Yukari Matsuishi [b], Toru Kawanishi [a], Takao Hayakawa [a]

[a] *Division of Biological Chemistry and Biologicals, National Institute of Health Science, 1-18-1, Kamiyoga, Setagaya-ku, Tokyo 158-8501, Japan*
[b] *CREST, Japan Science and Technology Agency (JST), Japan*

Received 17 May 2005; received in revised form 17 July 2005; accepted 25 July 2005
Available online 5 October 2005

Abstract

We developed an efficient and convenient strategy for protein identification and glycosylation analysis of a small amount of unknown glycoprotein in a biological sample. The procedure involves isolation of proteins by electrophoresis and mass spectrometric peptide/glycopeptide mapping by LC/ion trap mass spectrometer. For the complete glycosylation analysis, proteins were extracted in intact form from the gel, and proteinase-digested glycoproteins were then subjected to LC/multistage tandem MS (MS^n) incorporating a full mass scan, in-source collision-induced dissociation (CID), and data-dependent MS^n. The glycopeptides were localized in the peptide/glycopeptide map by using oxonium ions such as $HexNAc^+$ and $NeuAc^+$, generated by in-source CID, and neutral loss by CID-MS/MS. We conducted the search analysis for the glycopeptide identification using search parameters containing a possible glycosylation at the Asn residue with *N*-acetylglucosamine (203 Da). We were able to identify the glycopeptides resulting from predictable digestion with proteinase. The glycopeptides caused by irregular cleavages were not identified by the database search analysis, but their elution positions were localized using oxonium ions produced by in-source CID, and neutral loss by the data-dependent MS^n. Then, all glycopeptides could be identified based on the product ion spectra which were sorted from data-dependent CID-MS^n spectra acquired around localized positions. Using this strategy, we successfully elucidated site-specific glycosylation of Thy-1, glycosylphosphatidylinositol (GPI)-anchored proteins glycosylated at Asn23, 74, and 98, and at Cys111. High-mannose-type, complex-type, and hybrid-type oligosaccharides were all found to be attached to Asn23, 74 and 98, and four GPI structures could be characterized. Our method is simple, rapid and useful for the characterization of unknown glycoproteins in a complex mixture of proteins.

Keywords: Glycoprotein; LC/MS; Ion trap mass spectrometer; In-source CID; Thy-1

1. Introduction

Glycosylation is one of the most abundant post-translational modifications of proteins [1]. Most glycoproteins exist in heterogeneous forms due to their carbohydrate heterogeneity at multiple glycosylation sites. Because heterogeneity at each glycosylation site can be associated with many biological functions [2,3], it is necessary to analyze the oligosaccharide structures at each glycosylation site.

Mass spectrometric peptide/glycopeptide mapping by liquid chromatography coupled with electrospray ionaization tandem mass spectrometry (LC/ESI-MS/MS) is now used for characterization of glycoproteins [4,5]. Site-specific glycosylation of some gel-separated glycoproteins can be analyzed by in-gel proteinase digestion followed by MS; this method, however, gives unsatisfactory results due to a lower recovery of some glycopeptides from the gel [6–8]. For

* Corresponding author. Tel.: +81 3 3700 1141; fax: +81 3 3707 6950.
E-mail address: nana@nihs.go.jp (N. Kawasaki).

0021-9673/$ – see front matter © 2005 Elsevier B.V. All rights reserved.
doi:10.1016/j.chroma.2005.07.100

complete site-specific glycosylation analysis, all glycopeptide fragments should be recovered from the gel. Hence, the extraction of a whole glycoprotein from the gel before proteinase digestion would be more reasonable than in-gel digestion. Additionally, the poor ionization efficiency of glycopeptides makes it difficult to analyze the glycosylation of glycopeptides in a complex mixture of peptides [6,9]. The glycopeptide-specific method is required for mass spectrometric peptide/glycopeptide mapping.

A precursor ion scan using triple quadrupole-type mass spectrometer is favorably used for analysis of glycopeptides [10–13]. However, this method requires repetitive analysis for the protein identification and glycosylation analysis, as it monitors carbohydrate marker ions such as $HexNAc^+$ and $Hex\text{-}HexNAc^+$ fragmented from glycopeptides by collision-induced dissociation (CID)-MS/MS, and does not provide product ion spectra of non-glycosylated peptides. As such, additional analysis would not be possible for small quantities of proteins, including gel-separated glycoproteins. As an alternative method, we have previously demonstrated peptide/glycopeptide mapping using quadrupole time-of-flight mass spectrometer, by which product ions arise from both peptides and carbohydrates [14]. Using oxonium ions as marker ions, we can sort out product ion spectra of glycopeptides from a number of product ion spectra of peptides, and can determine the amino acid sequences of glycopeptides, glycosylation sites, and monosaccharide composition in a single analysis. Recently, ion trap mass spectrometry (ITMS), which is capable of data-dependent multistage tandem MS (MS^n), has been found to be preferable for use in glycosylation analysis of glycopeptides [15,16]. Glycopeptide-specific detection by precursor ion scan and data-dependent scan cannot be used for glycosylation analysis by ITMS due to the low mass cut-off system. Instead, oxonium ions fragmented by in-source CID are used for the localization of glycopeptides in the peptide/glycopeptide map [3,17]. It has recently been reported that peptide + GlcNAc ions originating from *N*-glycosylated peptides by MS^2 yield peptide b and y ions by further MS^n, and that the peptide sequence and *N*-glycosylation sites can be identified based on the peptide fragment ions [15,16,18]. In addition, another group has reported that glycopeptides can be identified in peptide/glycopeptide map by a search analysis using a database to which all possible cleavage products of the glycopeptides have been added in advance [19]. A combination of peptide/glycopeptide mapping with in-source CID, data-dependent CID-MS^n, and the database search analysis would enable protein identification, glycopeptide selection, and glycosylation analysis of a small amount of glycoprotein.

In the present study, we developed a strategy for the characterization of a small amount of unknown glycoprotein in a biological sample. An unknown glycoprotein was isolated by electrophoresis and extracted from the gel in an intact form. We used sodium dodecyl sulfate (SDS), which is effective for extracting proteins from the gel, and could be easily removed by adding cold acetone. The proteinase-digested glycoprotein was subjected to peptide/glycopeptide mapping, with the sequential scan consisting of a full mass scan, in-source CID, and data-dependent CID-MS^n. Using this method, we carried out site-specific glycosylation analysis of glycosylphosphatidylinositol (GPI)-anchored proteins in rat brain. A computer database search was used for the identification of a GPI-anchored protein and its *N*-glycosylation sites. In-source CID and data-dependent CID-MS/MS were also used for localization of peptides with *N*-glycan and GPI in the peptide/glycopeptide map. On the basis of their product ion spectra, we elucidated *N*-glycosylation at each glycosylation site and the structure of GPIs.

2. Experimental

2.1. Materials

Rat brains were purchased from Nippon SLC (Hamamatsu, Japan). Trypsin-Gold and endoproteinase Asp-N were purchased from Promega (Madison, WI, USA) and Wako Pure Chemical (Osaka, Japan), respectively. Phosphatidylinositol-specific phospholipase C (PIPLC) from *Bacillus cereus* were purchased from Molecular Probes (Eugene, OR, USA). All other chemicals used were of the highest purity available.

2.2. Sodium dodecyl sulfate-polyacrylamide gel electrophoresis (SDS-PAGE) of PIPLC-treated GPI-anchored proteins

PIPLC-treated GPI-anchored proteins were prepared from rat brain utilizing Triton X-114 phase partition and PIPLC digestion [20,21]. Two whole rat brains (2.8 g, Wistar, male, 3 weeks) were homogenized in cold acetone and centrifuged for 10 min at 4 °C. The precipitate was then homogenized in $CHCl_3$: methanol (2:1, v/v) and centrifuged for 10 min at 4 °C. After being washed with methanol, the pellet was homogenized in 50 mM Tris–HCl (pH 7.4) containing 150 mM NaCl, 1 mM ethylenediaminetetraacetic acid (EDTA), and 1 mM phenylmethylsulfonyl fluoride (PMSF), and centrifuged at 10,000 × *g* at 4 °C for 20 min. The pellet was resuspended in the same buffer with an additional 2% Triton X-114 (v/v), and stirred at 4 °C for 16 h. After centrifugation at 10,000 × *g* at 4 °C for 20 min, the supernatant was subjected to Triton X-114 phase-partitioning at 37 °C for 10 min. The detergent phase was resuspended with an equal volume of 50 mM Tris–HCl (pH 7.4) containing 150 mM NaCl. Solubilized membrane proteins in the detergent phase were precipitated with cold acetone and were resuspended in 400 μl of 50 mM Tris–HCl (pH 7.4). Following the addition of PIPLC (1 U), the suspension was incubated at 37 °C for 18 h. The suspension was resubjected to Triton X-114 phase-partitioning, and PIPLC-treated GPI-anchored proteins were precipitated with cold acetone from the aqueous phase. PIPLC-treated GPI-anchored proteins obtained from

50 mg of rat brain were separated by SDS-PAGE (12.5%) after carboxyamidomethylation [22].

2.3. Extraction and digestion of gel-separated proteins

The protein in gel band was extracted with 20 mM Tris–HCl containing 1% SDS by shaking vigorously overnight after breaking down the gel into small bits. The extract was filtered with Ultrafree-MC (0.22 μm, Millipore, Bedford, USA), and the protein was precipitated by adding cold acetone. The precipitate was digested with trypsin (1 μg) in 20 μl of 0.1 M Tris–HCl (pH8.0) at 37 °C for 16 h, or with Asp-N (0.4 μg) in 20 μl of 5 mM Tris–HCl (pH 7.5) at 37 °C overnight.

2.4. LC/MS^n

Proteolytic peptides were separated by a Magic C18 column (50 mm × 0.2 mm, 3 μm, Michrom BioResources, Auburn, CA, USA) with a Paradaim MS4 HPLC system (Michrom BioResources Inc., Auburn, CA, USA) consisting of pump A: 0.1% formic acid and 2% acetonitrile, and pump B: 0.1% formic acid and 90% acetonitrile. Separation was performed with a linear gradient of 5–65% of pump B in 40 min after 5% in 10 min of pump B at a flow rate 3 μl/min. Mass spectra were recorded by Finnigan LTQ (Thermo Electron, San Jose, CA, USA) with the sequential scan: a full mass scan (*m*/*z* 300–2000), a full mass scan with in-source CID (*m*/*z* 80–500, collision energy: 50 V), and data-dependent CID-MS^n for most intense ions at each scan with dynamic exclusion for 30 s. Scan time (*m*/*z* 300–2000) is approximately 0.1 s. The operating condition used for LC/ITMS was as follows: tube lens offset of 130 V, capillary voltage of 2.0 kV, capillary temperature of 200 °C.

2.5. Computer database search analysis

All product ions obtained by LC/ITMS were subjected to the computer database search analysis with the TurboSEQUEST search engine (Thermo Electron, San Jose, CA, USA). We used the NCBI database (rat, updated at February 2003) and following search parameters: a static modification of carboxyamidomethylation (57 Da) at Cys, a possible modification of GlcNAc (203 Da) at Asn, and trypsin used for digestion.

3. Results

3.1. Extraction of whole proteins from the gel

Rat brain PIPLC-treated GPI-anchored proteins were separated by SDS-PAGE (Fig. 1), and the most noticeable band at 20–25 kDa was cut off from the gel and crushed. The gel pieces were shaken vigorously in 1% SDS, and the extracted protein was precipitated with cold acetone to remove SDS.

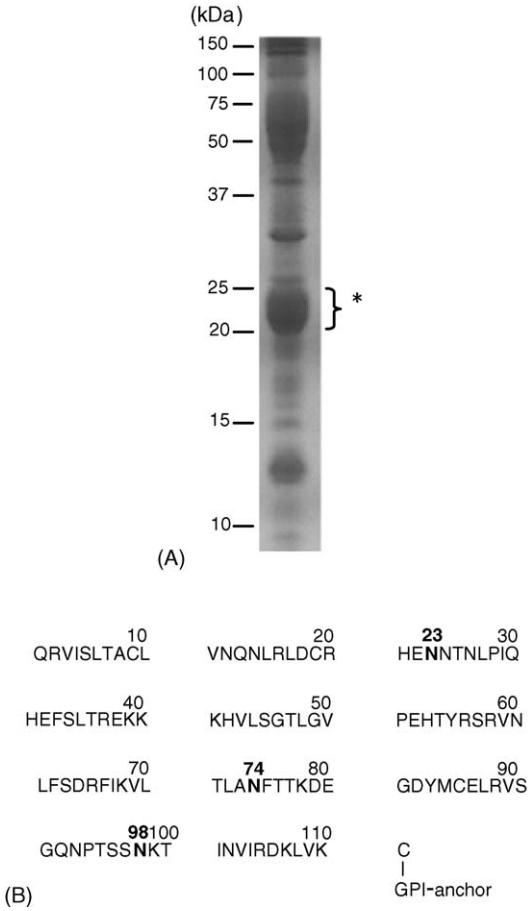

Fig. 1. (A) SDS-PAGE of PIPLC-treated GPI-anchored proteins from rat brain. (B) Amino acid sequence of rat Thy-1. *N*-Glycosylation sites are indicated by bold face. The protein at 20–25 kDa indicated by asterisk was subjected to the glycosylation analysis in this study.

We checked the recovery of the protein at 20–25 kDa by comparing the fluorescence intensity (Ex 633 nm/Em 670 nm) of the proteins at 20–25 kDa visualized by Coomassie staining before and after extraction. Approximately 55% of the protein at 20–25 kDa could be recovered from the gel (data not shown). The protein was digested with trypsin and subjected to the sequential scan consisting of full mass scans with and without in-source CID and data-dependent MS^n by LC/ITMS for protein identification and glycosylation analysis.

3.2. Database search analysis

Fig. 2(A) shows the peptide/glycopeptide map of the trypsin-digested protein at 20–25 kDa. First, all product ions generated by data-dependent MS^n were used for the database search analysis. Using search parameters described in Section 2.5, the protein was identified as Thy-1, a glycoprotein containing three *N*-glycosylation sites at Asn23, 74, and 98, and a GPI attachment site at Cys111. The search analysis also suggested the glycosylation at Asn74 and 98, with elution positions of 34 min (peak T6, Val69-Lys78) and 3.5 min (peak T1, Val89-Lys99), respectively (Fig. 2(A)). Although

Table 1
Glycosylation analysis of rat brain Thy-1

Glycosylation site	Carbohydrate composition[a]				Theoretical carbohydrate mass[b]	Trypsin					Asp-N				
	dHex	Hex	HexNAc	NeuAc		Observed *m/z*	Charge state	Peak number	Amino acid residue[c]	Theoretical *m/z*[b]	Observed *m/z*	Charge state	Peak number	Amino acid residue[c]	Theoretical *m/z*[b]
Asn23	0	5	2	0	1234.43	845.33	3	T3	H21-H31 (1315.63)	845.03	799.47	3	A3	E22-H31 (1178.57)	799.34
						937.27	3	T4	H21-F33 (1591.74)	937.06	1198.69	2	A3	E22-H31 (1178.57)	1198.50
						1405.81	2	T4	H21-F33 (1591.74)	1405.09	949.60	3	A3	N23-T36 (1626.80)	948.75
											1423.40	2	A3	N23-T36 (1626.80)	1422.62
	0	6	2	0	1396.49	899.49	3	T3	H21-H31 (1315.63)	899.04	853.54	3	A3	E22-H31 (1178.57)	853.36
						1348.35	2	T3	H21-H31 (1315.63)	1348.06	1279.66	2	A3	E22-H31 (1178.57)	1279.53
						942.16	3	T3	H21-E32 (1444.67)	942.06	1211.52	2	A5	E22-Q30 (1041.51)	1211.00
						991.37	3	T5	H21-F33 (1591.74)	991.08					
						1486.40	2	T5	H21-F33 (1591.74)	1486.12					
	0	3	5	0	1519.57						1044.43	3	A3	N23-T36 (1626.80)	1043.79
	0	7	2	0	1558.54	996.41	3	T3	H21-E32 (1444.67)	996.07	907.59	3	A3	E22-H31 (1626.80)	907.37
											1361.03	2	A3	E22-H31 (1178.57)	1360.56
	1	3	5	0	1665.62						1093.32	3	A3	N23-T36 (1626.80)	1092.48
	1	5	4	0	1786.65						1133.80	3	A3	N23-T36 (1626.80)	1132.82
	0	6	3	1	1890.66						1168.51	3	A4	N23-T36 (1626.80)	1167.49
	1	6	4	0	1948.70						1187.21	3	A3	N23-T36 (1626.80)	1186.84
Asn74	1	2	3	0	1405.52	1026.26	3	T6	V59-F75 (1996.12)	1026.18					
	0	5	2	0	1234.43	949.52	2	T2	A73-K78 (680.35)	949.39	995.71	3	A7	D64-K78 (1766.01)	995.15
						1162.72	2	T6	V69-K78 (1106.62)	1162.53					
	1	4	3	0	1421.52	1043.45	2	T2	A73-K78 (680.35)	1042.94					
	1	3	4	0	1462.54	1063.68	2	T2	A73-K78 (680.35)	1063.45					
						1276.61	2	T6	V69-K78 (1106.62)	1276.58					
	1	5	3	0	1583.57	1124.18	2	T2	A73-K78 (680.35)	1123.96					
						1337.64	2	T6	V69-K78 (1106.62)	1337.10					
	1	3	5	0	1665.62	1165.13	2	T2	A73-K78 (680.35)	1164.99	1272.15	2	A4	T71-K78 (894.48)	1272.05
						919.71	3	T6	V69-K78 (1106.62)	919.09	1139.79	3	A7	D64-K78 (1766.01)	1138.88
						1378.19	2	T6	V69-K78 (1106.62)	1378.12					
	2	5	3	0	1729.63	1197.53	2	T2	A73-K78 (680.35)	1196.99					
	2	4	4	0	1770.66	1217.67	2	T2	A73-K78 (680.35)	1217.51					
						1430.71	2	T6	V69-K78 (1106.62)	1430.64					
	1	5	4	0	1786.65	1226.38	2	T2	A73-K78 (680.35)	1225.50					
						960.01	3	T6	V69-K78 (1106.62)	959.43					
						1439.05	2	T6	V69-K78 (1106.62)	1438.64					
	1	4	5	0	1827.68	973.79	3	T6	V69-K78 (1106.62)	973.10					
	2	5	4	0	1932.71	1298.75	2	T2	A73-K78 (680.35)	1298.53	1228.18	3	A7	D64-K78 (1766.01)	1227.91
						1008.71	3	T6	V69-K78 (1106.62)	1008.11					
						1512.21	2	T6	V69-K78 (1106.62)	1511.67					
	1	6	4	0	1948.70	1306.81	2	T2	A73-K78 (680.35)	1306.53					
						1013.98	3	T6	V69-K78 (1106.62)	1013.45					
	0	4	5	1	1972.71						1241.91	3	A7	D64-K78 (1766.01)	1241.25
	2	4	5	0	1973.73	880.04	3	T2	A73-K78 (680.35)	879.70	1241.84	3	A7	D64-K78 (1766.01)	1241.59
						1319.24	2	T2	A73-K78 (680.35)	1319.04					
						1022.43	3	T6	V69-K78 (1106.62)	1021.79					
						1532.49	2	T6	V69-K78 (1106.62)	1532.49					

	1	6	3	1	2036.72	1043.24	3	T7	V69-K78 (1106.62)	1042.78					
	1	5	4	1	2077.75	1057.08	3	T7	V69-K78 (1106.62)	1056.46					
	2	6	4	0	2094.76	1062.65	3	T6	V69-K78 (1106.62)	1062.13	1282.43	3	A7	D64-K78 (1766.01)	1281.93
	1	4	5	1	2118.77	1070.38	3	T7	V69-K78 (1106.62)	1070.14					
	2	5	5	0	2135.79	1076.32	3	T6	V69-K78 (1106.62)	1075.81					
	1	6	4	1	2239.80	1110.97	3	T7	V69-K78 (1106.62)	1110.48					
	3	5	5	0	2281.85	1124.78	3	T6	V69-K78 (1106.62)	1124.49					
	1	7	5	0	2313.84	851.76	4	T6	V69-K78 (1106.62)	851.62					
	1	4	6	1	2321.85	1138.16	3	T7	V69-K78 (1106.62)	1137.83					
	2	5	6	1	2629.96	1241.13	3	T7	V69-K78 (1106.62)	1240.53					
Asn98	0	5	2	0	1234.43	1168.34	2	T1	V89-K99 (1117.54)	1167.99	912.24	3	A2	E86-K99 (1515.76)	911.74
											1367.31	2	A2	E86-K99 (1515.76)	1367.10
											930.26	3	A3	Q92-R105 (1570.84)	930.10
											1021.28	3	A3	E86-N102 (1843.94)	1021.13
											1011.53	3	A4	T95-K110 (1815.06)	1010.81
											1516.43	2	A4	T95-K110 (1815.06)	1516.75
											1144.21	3	A5	E86-R105 (2212.18)	1143.88
	0	3	4	0	1316.49	1209.79	2	T1	V89-K99 (1117.54)	1209.02					
	0	3	5	0	1519.57	1310.68	2	T1	V89-K99 (1117.54)	1310.56	1007.10	3	A2	E86-K99 (1515.76)	1006.78
											1106.39	3	A4	T95-K110 (1815.06)	1106.55
											1239.21	3	A5	E86-R105 (2212.18)	1238.92
	2	3	4	0	1608.60						951.28	3	A4	G91-N102 (1259.61)	951.08
											1426.22	2	A4	G91-N102 (1259.61)	1426.11
	1	4	4	0	1624.60	951.37	3	T3	S96-D106 (1245.67)	951.76					
	0	5	4	0	1640.59	1371.84	2	T1	V89-K99 (1117.54)	1371.07	960.04	4	A5	E86-R105 (2212.18)	959.70
											1279.69	3	A5	E86-R105 (2212.18)	1279.26
	0	5	3	1	1728.61						1176.27	3	A4	T95-K110 (1815.06)	1176.23
	0	5	4	0	1640.59						1146.70	3	A4	T95-K110 (1815.06)	1146.89
	1	6	3	0	1745.62						1082.52	3	A2	E86-K99 (1515.76)	1082.13
											1181.80	3	A4	T95-K110 (1815.06)	1181.90
											986.38	4	A5	E86-R105 (2212.18)	985.96
											1314.72	3	A5	E86-R105 (2212.18)	1314.27
	1	5	4	0	1786.65						1195.47	3	A4	T95-K110 (1815.06)	1195.57
											996.54	4	A5	E86-R105 (2212.18)	996.21
											1328.49	3	A5	E86-R105 (2212.18)	1327.95
	1	5	3	1	1874.67						1018.89	4	A6	E86-R105 (2212.18)	1018.22
	0	6	3	1	1890.66	1496.18	2	T1	V89-K99 (1117.54)	1496.10	1230.24	3	A4	T95-K110 (1815.06)	1230.24
											1022.70	4	A6	E86-R105 (2212.18)	1022.22
	2	5	4	0	1932.71	1517.35	2	T1	V89-K99 (1117.54)	1517.13					
	1	6	4	0	1948.70	1525.78	2	T1	V89-K99 (1117.54)	1525.12	1150.13	3	A2	E86-K99 (1515.76)	1149.83
											1249.75	3	A4	T95-K110 (1815.06)	1249.59
											1259.45	3	A3	E86-N102 (1843.94)	1259.22
											1037.27	4	A5	E86-R105 (2212.18)	1036.73
											1382.34	3	A5	E86-R105 (2212.18)	1381.97
	1	6	3	1	2036.72						1059.07	4	A6	E86-R105 (2212.18)	1058.73
	0	6	4	1	2093.74						1298.06	3	A4	T95-K110 (1815.06)	1297.94
											1073.37	4	A6	E86-R105 (2212.18)	1072.99

[a] dHex, deoxyhexose; Hex, hexose; HexNAc, *N*-acetylhexosamine; NeuAc, *N*-acetylneuramic acid.

[b] Monoisotopic value.

[c] Theoretical peptide mass is indicated in parenthesis.

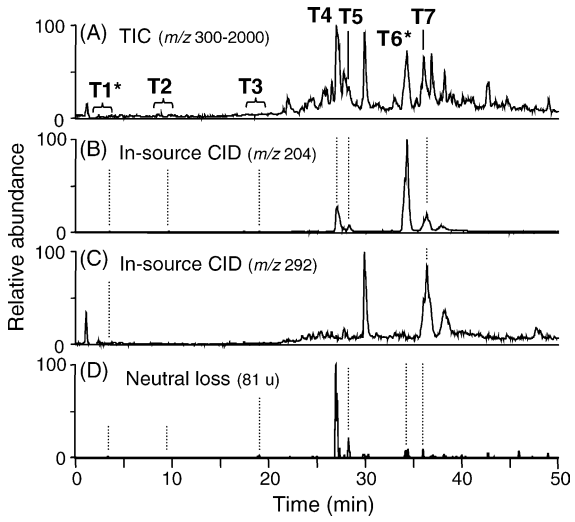

Fig. 2. Total ion chromatogram (TIC) of trypsin-digested protein at 20–25 kDa (*m/z* 300–2000) (A), mass chromatograms from TIC with ion-source CID of *m/z* 204 (B) and 292 (C), and neutral loss chromatogram of 81 u by data-dependent CID-MS/MS (D). Asterisks mean the peak of glycopeptides identified by the database search analysis.

the glycopeptide Val89-Lys99 contains two Asn residues, Asn93 and 98, only Asn98 was identified as a glycosylation site because of detection of b and y ions modified with GlcNAc at Asm98.

Next, to study the site-specific glycosylation at Asn74 and 98, product ion spectra of glycopeptides were sorted from the numbers of product ion spectra acquired around peak T6 and T1. We sorted out product ion spectra of glycopeptides using B series ions, such as $Hex_1HexNAc_1^+$ and $Hex_2HexNAc_1^+$ (*m/z* 366 and 528) originated from glycopeptides by CID-MS/MS, as marker ions [23]. We could sort out 14 product ion spectra originated from glycopeptide Val69-Lys78 around peak T6. The monosaccharide compositions of *N*-glycans at Val69-Lys78 were calculated as $dHex_{0–3}Hex_{2–7}HexNAc_{2–5}$ on the basis of the *m/z* values of their molecular ions and the theoretical mass of the peptide. Likewise, seven product ion spectra originated from glycopeptide Val89-Lys99 were sorted from those around peak T1, and their monosaccharide compositions were estimated as $dHex_{0–2}Hex_{3,5,6}HexNAc_{2–5}NeuAc_{0,1}$ (Table 1). Glycosylation at Asn74 and 98 were elucidated by a detailed examination of these product ion spectra as follows.

3.2.1. Analysis of the glycosylation at Asn74 of peptide Val69-Lys78

Fig. 3(A) shows a product ion spectrum of the glycopeptide Val69-Lys78 at 34.52 min. Its precursor ion is the doubly charged ion at *m/z* 1512.2. Many product ions generated by cleavages of glycosidic linkages can be observed in this product ion spectrum. The most intense ion at *m/z* 1311 is assigned to a peptide bearing the reducing end of GlcNAc, which was caused by glycosidic linkage cleavage of *N*-linked oligosaccharide. Fig. 3(B) is the product ion spectrum of the peptide + GlcNAc ion at *m/z* 1311. The b and y ions generated by cleavages of the peptide backbone prove that this glycopeptide is the peptide Val69-Lys78 glycosylated at Asn74.

The molecular weight of the carbohydrate moiety can be calculated as 1933.8 Da by subtracting the theoretical mass of the peptide (1106.6 Da) from the calculated glycopeptide mass (3022.4 Da). Consequently, the monosaccharide composition can be estimated as $dHex_2Hex_5HexNAc_4$. In the product ion spectrum (Fig. 3(A)), B ions corresponding to $dHex_1Hex_1HexNAc_1$ ($B_{2\alpha}$) and $dHex_1Hex_2HexNAc_1$ ($B_{3\alpha}$) were detected at *m/z* 512 and 674, respectively. These results indicate that one of two dHex, which are likely to be Fuc, attaches to Gal-GlcNAc at the non-reducing end in a similar manner as the Lewis a/x antigen (Gal-(Fuc-)GlcNAc-), or the blood group H-determinant (Fuc-Gal-GlcNAc-). The product ion at *m/z* 350 produced from the triply charged precursor ion at *m/z* 1008.7 corresponded to $dHex_1HexNAc_1$ (data not shown), suggesting that Fuc attaches to GlcNAc like the Lewis a/x antigen (Gal-(Fuc-)GlcNAc-). The attachment site of the other Fuc can be deduced at inner trimannosyl core GlcNAc from the observation of Y ions at *m/z* 1457, 1660, and 1822, which correspond to Val69-Lys78 plus $dHex_1HexNAc_1$ ($Y_{1\alpha}$), $dHex_1HexNAc_2$ ($Y_{2\alpha}$), and $dHex_1Hex_1HexNAc_2$ ($Y_{3\alpha/3\beta/3\gamma}$), respectively. In addition, the product ion at *m/z* 1411 resulting from the precursor ion at *m/z* 1512.2 by loss of 101.6 u (HexNAc), suggests a linkage of non-substituted HexNAc at the non-reducing terminal end. Together with detection of the product ion at *m/z* 940 ($Y_{3\alpha/1\beta/3\beta}^+$, [GlcNAc-Man-GlcNAc-GlcNAc-peptide+H]$^{2+}$), it can be deduced that this HexNAc is a bisecting GlcNAc attached to the core mannose residue via a β1–4 linkage. From these product ions, we could deduce two oligosaccharide structures. One is the structure indicated in Fig. 3(A), inset, and the other is one containing a Gal-Gal-(Fuc-)GlcNAc-Man-branch instead of a Gal-(Fuc-)GlcNAc-Man-branch. Detection of Gal-(Fuc-)GlcNAc-Man$^+$ at *m/z* 674 but not Gal-Gal-(Fuc-)GlcNAc-Man$^+$ at *m/z* 836 suggests that this oligosaccharide structure can be assigned to the structure indicated in Fig. 3(A), inset.

The carbohydrate structures of the other glycopeptide Val69-Lys78 detected around peak T6 can be characterized as the high-mannose-type oligosaccharide (M5), complex-type oligosaccharides containing some partial structures such as inner core Fuc, bisecting GlcNAc, the Lewis a/x antigen, and blood group H-determinant, and hybrid-type oligosaccharides (Table 1).

3.2.2. Analysis of the glycosylation at Asn98 of peptide Val89-Lys99

Fig. 4 shows one of the product ion spectra of the glycopeptide Val89-Lys99 at 3.47 min. Its precursor ion is the doubly charged ion at *m/z* 1525.8. The monosaccharide composition, $dHex_1Hex_6HexNAc_4$, can be estimated based on the calculated mass of the carbohydrate moiety (1950.0 Da) obtained by subtracting the mass of the theo-

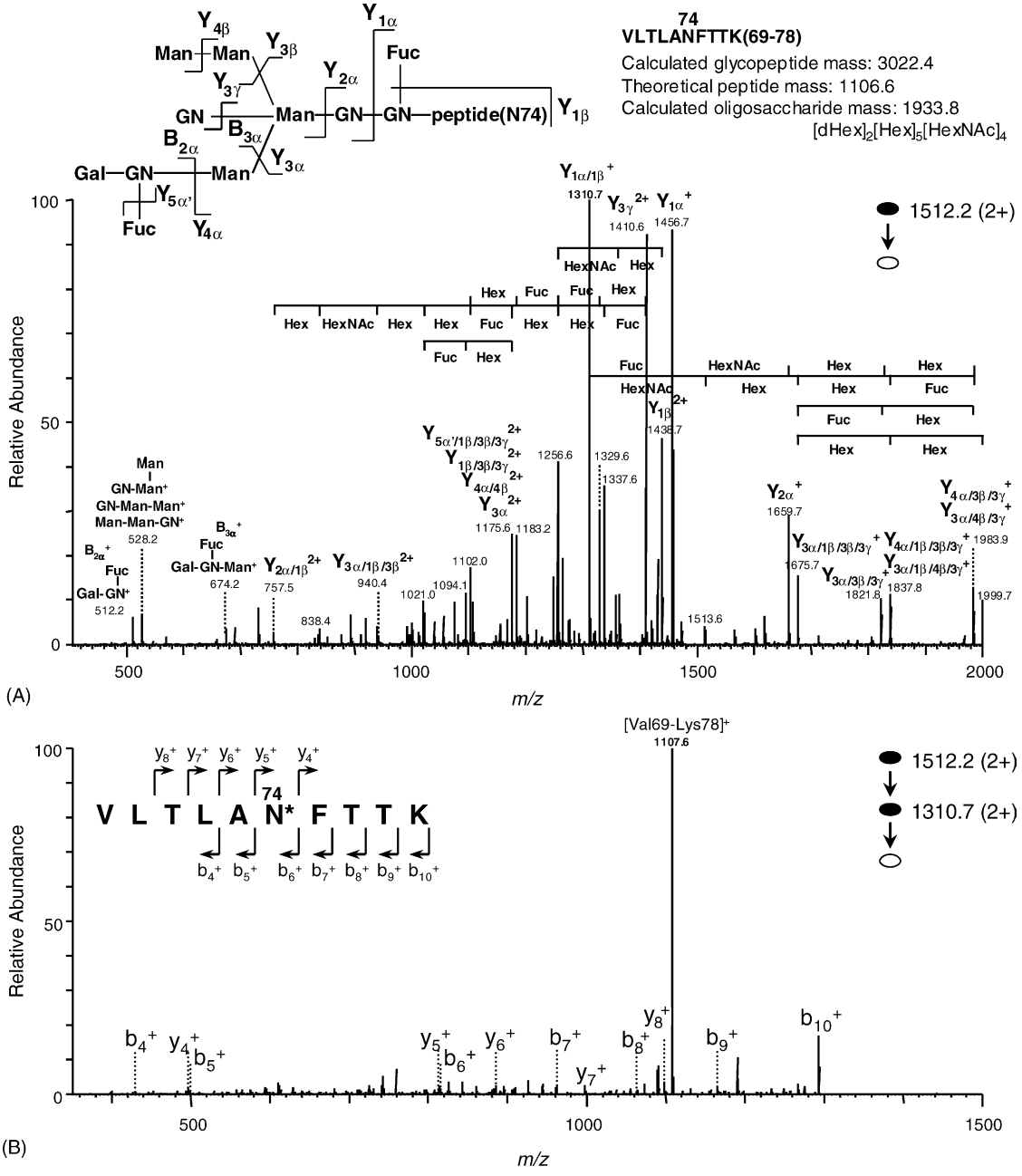

Fig. 3. (A) Product ion spectrum (MS^2) of the doubly charged glycopeptide precursor ion at *m/z* 1512.2 in peak T6. The glycopeptide Val69-Lys78 is glycosylated with oligosaccharide, $dHex_2Hex_5HexNAc_4$ at Asn74, and the inset is the deduced oligosaccharide structure. (B) MS^3 product ion spectrum derived from the doubly charged glycopeptide precursor ion at *m/z* 1512.2, followed by further fragmentation of the product ion at *m/z* 1310.7.

retical typtic peptide mass (1117.5 Da) from the calculated glycopeptide mass (3049.5 Da). Y ions corresponding to Val89-Lys99 plus $dHex_1HexNAc_1$ ($Y_{1\alpha}$), $dHex_1HexNAc_2$ ($Y_{2\alpha}$), and $dHex_1Hex_1HexNAc_2$ ($Y_{3\alpha/3\beta/3\gamma}$) detected at *m/z* 1468, 1671, and 1833, respectively, reveals that one Fuc residue is linked to the inner trimannosyl core GlcNAc. Additionally, the product ion at *m/z* 1424 suggests a linkage of non-substituted HexNAc at the non-reducing terminal end. Together with the product ions at *m/z* 945 and 1890, it can be deduced that this HexNAc is a bisecting GlcNAc that attaches to a core mannose residue via a β1–4 linkage. On the basis of the product ions at *m/z* 487, 528 and 1380, corresponding to Hex_3 ($B_{2\beta}$), $Hex_2HexNAc_1$ ($B_{3\alpha}$), and $Hex_6HexNAc_2$ ($B_{4\alpha}$), the oligosaccharide structure was characterized as a hybrid-type oligosaccharide (Fig. 4, inset).

The carbohydrate structures of the other glycopeptide Val89-Lys98 detected around peak T1 are characterized as high-mannose-type oligosaccharide (M5), complex-type, and hybrid-type oligosaccharides, which include bisecting GlcNAc and Lewis a/x structures (Table 1).

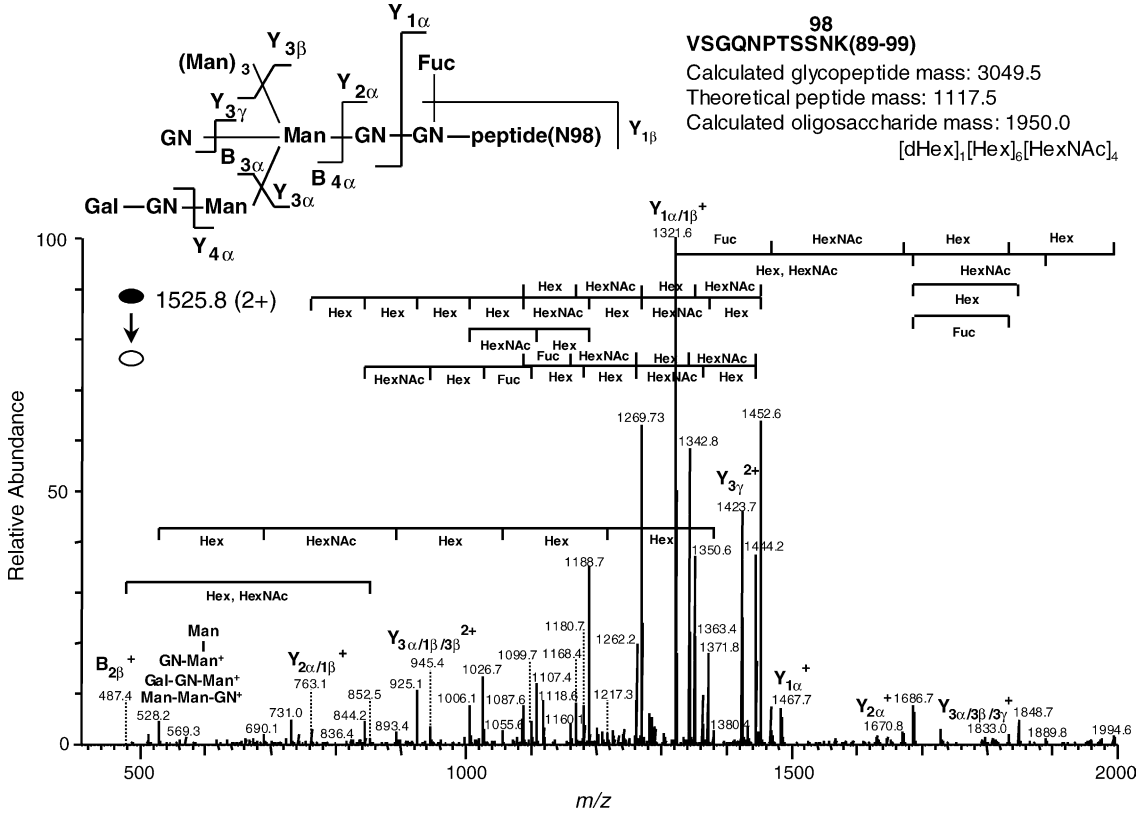

Fig. 4. Product ion spectrum of the doubly charged glycopeptide precursor ion at *m/z* 1525.8 in peak T1. The glycopeptide Val89-Lys99 is glycosylated with the oligosaccharide, $dHex_1Hex_6HexNAc_4$ at Asn98, and the inset is the deduced oligosaccharide structure.

3.3. Detection of glycopeptides by in-source CID and CID-MS/MS

Glycopeptides containing Asn23 could not be identified by the database search analysis. Therefore, we first localized all glycopeptides in the peptide/glycopeptide map using oxonium marker ions generated by in-source CID. Fig. 2(B and C) shows mass chromatograms of oxonium marker ions, $HexNAc^+$ (*m/z* 204) and $NeuAc^+$ (*m/z* 292), respectively. The mass chromatogram of *m/z* 204 indicates that the glycopeptides were localized around 3.7, 9.7, 19.1, 27.2, 28.4 34.3, 36.3, and 37.8 min. The mass chromatogram of *m/z* 292 suggests that the glycopeptides bearing NeuAc were localized around 3.7, 30.0, 36.4, and 38.2 min. In addition to the localization of glycopeptides by in-source CID, we monitored neutral loss caused by data-dependent CID-MS/MS. The neutral loss chromatogram of 81 u indicates the localization of doubly charged glycopeptides ions with Hex at the non-reducing ends. The elution positions of the localized glycopeptides by neutral loss are almost identical to those by in-source CID. Second, for confirmation of the elution position of glycopeptides and characterization of the carbohydrate moiety, we sorted the product ion spectra of glycopeptides from enormous numbers of data-dependently acquired product ion spectra around localized glycopeptides by using oligosaccharide oxonium ions as marker ions. Consequently, the locations of glycopeptides were confirmed in peak T1-6 (Fig. 2(A)). The peaks T1 and 6 correspond to the location of glycopeptides identified by the database search as Val89-Lys99 and Val69-Lys78, respectively. Four glycopeptide peaks were newly sorted by in-source CID and data-dependent CID-MS/MS. Structural assignment of the glycopeptides in these peaks was carried out using their MS^n spectra as follows.

3.3.1. Analysis of the glycosylation at Asn23 of peptide His21-Phe33

Fig. 5(A) shows one of the product ion spectra of the glycopeptide His21-Phe33 in peak T4. Its precursor ion is the triply charged ion at *m/z* 937.3. The intense product ion at *m/z* 899 is assigned to a doubly charged ion of peptide plus GlcNAc on the basis of Y series ions. The region of His21-Phe33 containing Asn23 in Thy-1 was suggested as the peptide moiety of this glycopeptide, 1593.3 Da, by the FindPept tool available on the internet (ExPASY Proteomics tools, Swiss Institute of Bioinformatics, http://us.expasy.org/tools/findpept.html). We examined the data-dependently acquired product ion spectrum of the precursor ion at *m/z* 899 and found that the *m/z* values of b and y ions in the product ion spectrum were identical to those of predictable product ions originating from the peptide His21-Phe33 modified with HexNAc at Asn23 (Fig. 5(B)). From the calculated oligosaccharide mass (1235.1 Da) obtained by subtracting the theoretical typtic

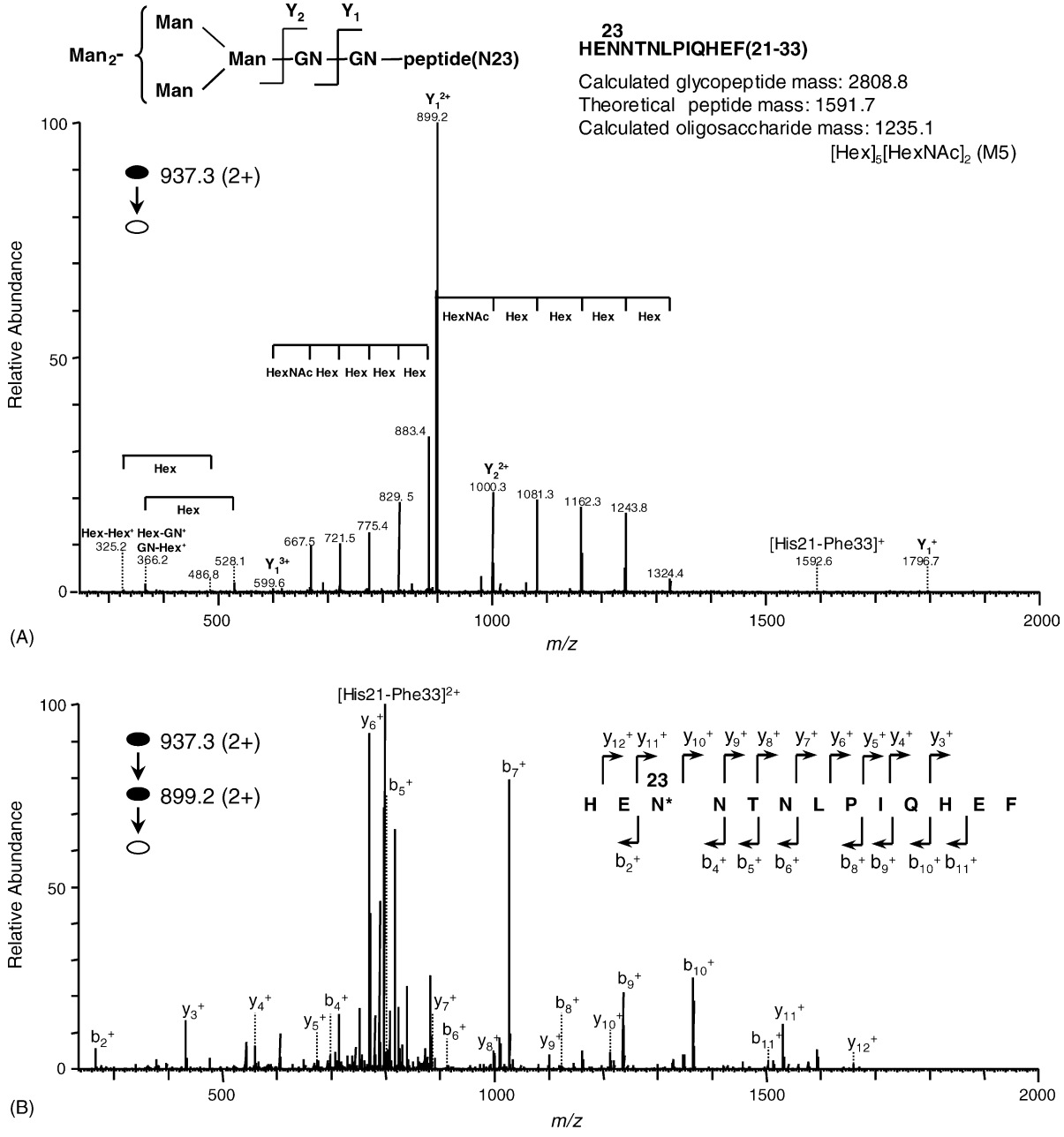

Fig. 5. (A) Product ion spectrum (MS^2) of the doubly charged glycopeptide precursor ion at *m/z* 937.3 in peak T4. The glycopeptide His21-Phe33 is glycosylated with oligosaccharide, $Hex_5HexNAc_2$ at Asn23, and the inset is the deduced oligosaccharide structure. (B) MS^3 product ion spectrum derived from a doubly charged glycopeptide precursor ion at *m/z* 937.3, followed by further fragmentation of the product ion at *m/z* 899.2.

peptide mass (1591.7 Da) from the calculated glycopeptide mass (2808.8 Da) together with product ions at *m/z* 366 and 528, it is indicated that this peptide carries $Hex_5HexNAc_2$, i.e. high-mannose-type oligosaccharide, M5. All product ion spectra in peak T4 revealed that peptides His21-Phe33 contain only high-mannose-type oligosaccharide (M5).

3.3.2. Analysis of glycopeptides in peaks T2, 3, 5, and 7

Similarly, product ion spectra of glycopeptides around peaks T2, 3, 5, and 7 were sorted by using oligosaccharide oxonium marker ions generated by MS/MS. In product ion spectra sorted out from around peak T2, the intense ion at *m/z* 884 was detected and assigned to a singly charged ion of a peptide plus GlcNAc. The peptide was suggested to be Ala73-Lys78 containing Asn74 by the FindPept tool. The monosaccharide composition can be estimated from the calculated mass of oligosaccharide moiety obtained by subtracting the theoretical mass of Ala73-Lys78 (680.35 Da) from calculated glycopeptide mass. Oligosaccharide structure of the glycopeptides is characterized based on their product

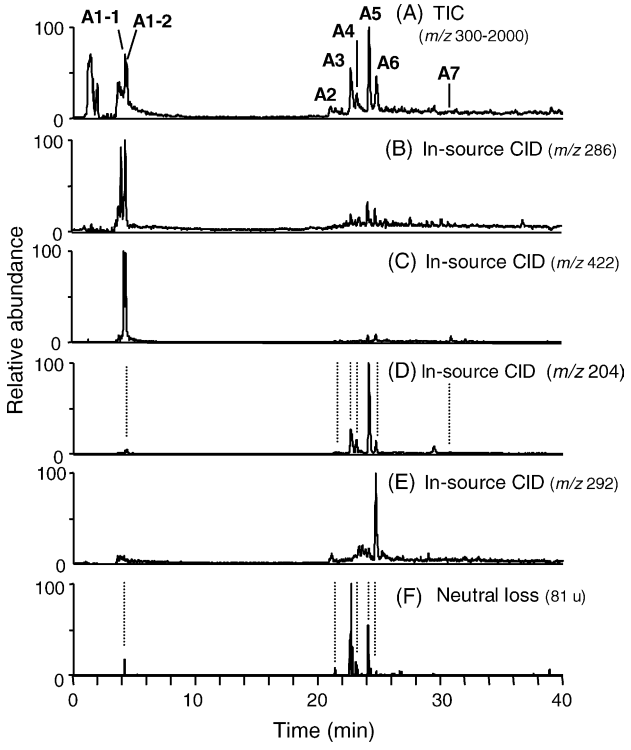

Fig. 6. Total ion chromatogram (TIC) of Asp-N digested protein at 20–25 kDa (*m/z* 300–2000) (A), mass chromatograms from TIC with in-source CID of *m/z* 286 (B), 422 (C), 204 (D), and 292 (E), and neutral loss chromatogram of 81 u by data-dependent CID-MS/MS (F).

ion spectra. Glycopeptides in peak T2 were characterized as Ala73-Lys78 glycosylated at Asn74 with *N*-glycans consisting of $dHex_{0–2}Hex_{3–6}HexNAc_{2–5}$. These *N*-glycans can be identified as high-mannose-type oligosaccharide (M5), and complex-type and hybrid-type oligosaccharides containing Fuc attached to inner trimannosyl core GlcNAc. Their structural assignments are summarized in Table 1. Glycopeptides in peak T3 can be identified as a mixture of peptide His21-His31 and His21-Glu32 glycosylated at Asn23, and Ser96-Asp106 glycosylated at Asn98. Asn23 was attached by high-mannose-type oligosaccharides, M5, 6, and 7, and Asn98 was occupied by *N*-glycan consisting of $dHex_1Hex_4HexNAc_4$ with a Lewis a/x structure as a partial structure. Glycopeptides in peak T5 were characterized as peptide His21-Phe33 glycosylated at Asn23 with high-mannose-type oligosaccharide, M6. Glycopeptides in peak T7 were assigned to be Val69-Lys78 glycosylated at Asn74 with *N*-glycans composed of $dHex_{1–2}Hex_{4–6}HexNAc_{3–6}NeuAc$.

3.4. Analysis of the GPI moiety of rat Thy-1

Since trypsin digestion provided Cys-GPI, which could not be retained on the C_{18} column, Asp-N digestion was also performed to obtain more hydrophobic peptides attached by GPI (GPI-peptides). Fig. 6(A) shows the peptide/glycopeptide map obtained by LC/ITMS of Asp-N digested Thy-1. We localize the GPI-peptides using marker ions, EtN-PO_4-Man^+ at *m/z* 286 and GlcN-inositol-PO_4^+ at *m/z* 422, originating from the core structure of the GPI moiety by in-source CID (EtN, ethanolamine; GlcN, glucosamine). Mass chromatograms of *m/z* 286 and 422 suggest the locations of the GPI-peptides to be around 4.2 (peak A1-1) and 4.4 min (peak A1-2) (Fig. 6(B and C)). Using product ions originated from GPI moiety, such as GlcN-inositol-PO_4^+ and PO_4-Man-$GlcN^+$ (*m/z* 422 and 404), as marker ions, four product ion spectra of GPI-peptides were sorted out from all product ion spectra around peaks A1-1 and 1-2. Their precursor ions were doubly charged ions at *m/z* 1132 and 1213 (peak A1-1), 1051 and 1151 (peak A1-2). Based on these product ion spectra, we characterized GPI-peptides as the peptide Asp106-Cys111 with a GPI core structure plus $Hex_{0–2}$, $HexNAc_{1–2}$ and PO_4-EtN.

Fig. 7(A) shows the product ion spectrum of the doubly charged GPI-peptide ion at *m/z* 1051 in peak A1-2. In addition to product ions at *m/z* 422, those originating from the GPI moiety were detected at *m/z* 404 (PO_4-Man-$GlcN^+$), 447 (EtN-PO_4-Man-$GlcN^+$), 650 (EtN-PO_4-(HexNAc-)Man-$GlcN^+$), 787 (peptide-EtN^+), 868 (peptide-EtN-PO_4^+), 1191 (peptide-EtN-PO_4-Man-Man^+), 1477 (peptide-EtN-PO_4-Man-Man-(EtN-PO_4-)Man^+), 1638 (peptide-EtN-PO_4-Man-Man-(EtN-PO_4-)Man-$GlcN^+$), and 1898 (peptide-EtN-PO_4-Man-Man-(EtN-PO_4-)Man-GlcN-inositol-PO_4^+). From these fragments, it can be deduced that this peptide is Asp106-Cys111 carrying the GPI, as indicated in the inset in Fig. 7(A).

The other GPI-peptide in peak A1-1 was characterized as having side chains; -Hex attached to M1, -PO_4-EtN and -HexNAc attached to M3, based on the product ion spectrum of the doubly charged precursor ion at *m/z* 1132 (data not shown). These two GPI structures are identical to those that have been previously reported [24].

Product ion spectra of doubly charged ion at *m/z* 1151 and 1213 suggested that they contained GPI which bear one HexNAc or two Hex in addition to GPI in Fig. 7(A) respectively. Fig. 7(B) shows the product ion spectra of the doubly charged precursor ions at *m/z* 1151 in peak A1-2. In addition to *m/z* 422, we detected product ions at *m/z* 366 (HexNAc-Man^+), 447 (EtN-PO_4-Man-$GlcN^+$), 650 (EtN-PO_4-(HexNAc-)Man-$GlcN^+$), 1229 (peptide-EtN-PO_4-(HexNAc-)Man^+), 1391 (peptide-EtN-PO_4-(HexNAc-)Man-Man^+), 1676 (peptide-EtN-PO_4-(HexNAc-)Man-Man-(EtN-PO_4-)Man^+), 1838 (peptide-EtN-PO_4-(HexNAc-)Man-Man-(EtN-PO_4-)Man-$GlcN^+$), and 1880 (peptide-EtN-PO_4-(HexNAc-)Man-Man-(EtN-PO_4-)(HexNAc-)Man^+). These fragment ions suggest the attachment of -HexNAc to Man1, and -PO_4-EtN and -HexNAc to Man3 as indicated in the inset of Fig. 7(B). Similarly, product ion spectra of the doubly charged precursor ion at *m/z* 1213 indicate the attachment of 2Hex and HexNAc to Man1 and Man3-PO_4-EtN (data not shown). To our knowledge, this is the first report of these two GPI structures in Thy-1.

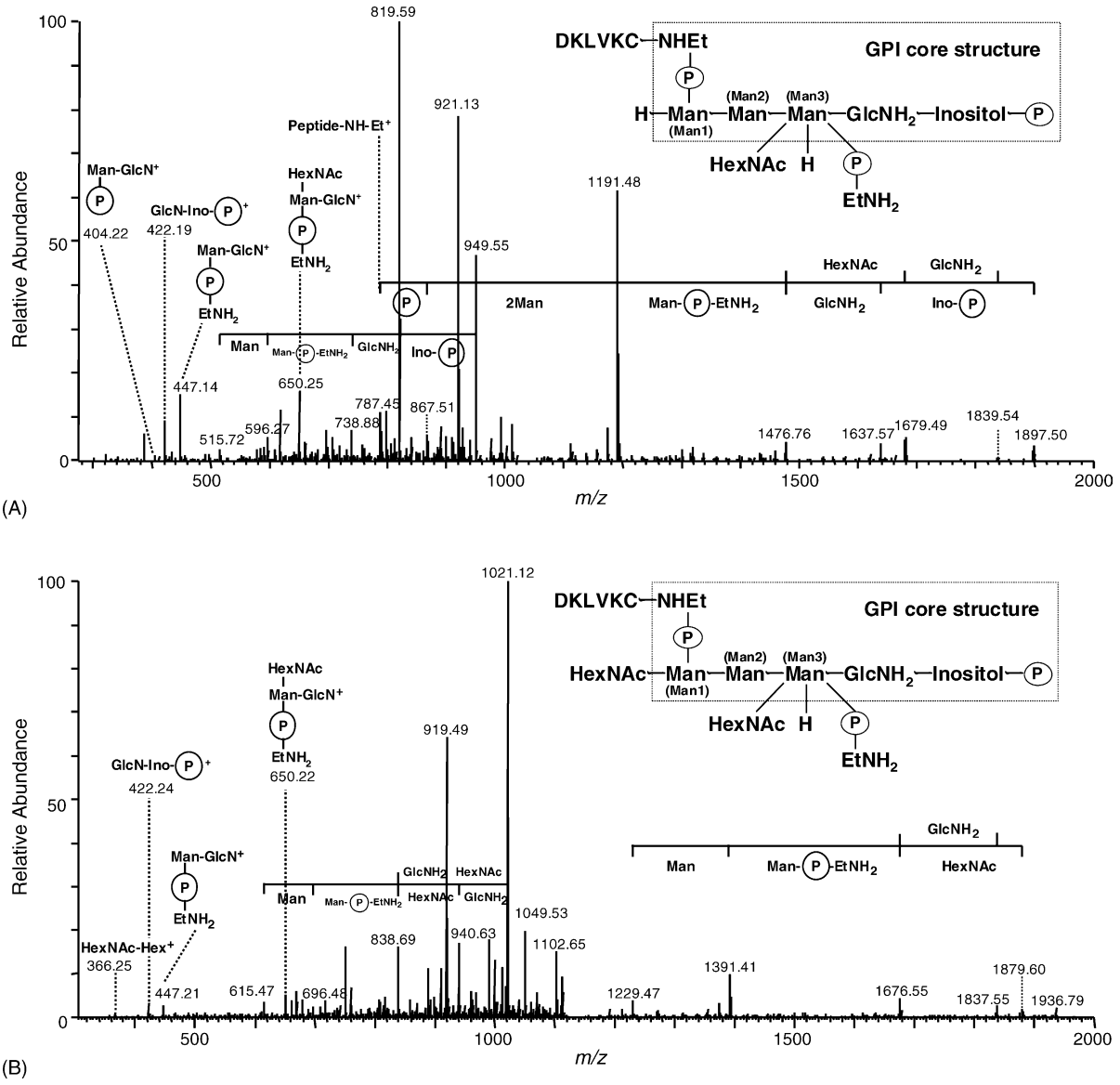

Fig. 7. Product ion spectra of the doubly charged GPI-peptide at *m/z* 1051 (A), and at *m/z* 1151 (B) in peak A1-2. The inset is the deduced structure of the GPI-peptide, and the core structure of GPI is the inside dashed line. Man, mannose; HexNAc, *N*-acetylhexosamine; $GlcNH_2$, glucosamine; $EtNH_2$-P, phosphorylethanolamine; Ino-P, inositol-phosphate.

3.5. Analysis of Asp-N digested Thy-1

Glycopeptides obtained by Asp-N digestion were also localized by in-source CID using marker ions at *m/z* 204 and 292 (Fig. 6(D and E)), and neutral loss of 81 u by data-dependent CID-MS/MS (Fig. 6(F)). Product ion spectra of glycopeptides were sorted by using B series ions as marker ions from those acquired around localized elution positions. Consequently, peaks A2-7 were identified as those of glycopeptides (Fig. 6(A)). The oligosaccharide structures in the glycopeptides were then characterized based on their product ion spectra (Table 1). In addition to the high-mannose-type oligosaccharides, M5, 6, and 7 deduced by LC/MS^n of tryptic digests, the oligosaccharide at Asn23 was characterized as $dHex_{0–1}Hex_{3,5,6}HexNAc_{3–5}NeuAc_{0,1}$, complex-type and hybrid-type oligosaccharides containing Lewis a/x or bisecting GlcNAc as a partial structure. Asn74 is attached by *N*-glycans with $dHex_{0–2}Hex_{3–6}HexNAc_{2,4,5}NeuAc_{0,1}$. They were high-mannose-type oligosaccharide, M5, complex-type oligosaccharides containing core Fuc and Lewis a/x as a partial structure, and hybrid-type oligosaccharides with core Fuc. Asn98 is occupied by high-mannose-type oligosaccharides, M5, and *N*-glycans with $dHex_{0–2}Hex_{3,5,6}HexNAc_{2–5}NeuAc_{0,1}$, hybrid-type oligosaccharides containing Lewis a/x or blood group H-determinant as a partial structure, which were found to be of greater diversity than those deduced by analysis of tryptic digests.

4. Discussion

In the present study, we have developed an efficient and convenient strategy for characterization, including protein identification and glycosylation analysis, of a small amount of unknown protein. We used gel electrophoresis, which is a powerful tool for separation of a small amount of protein from complex proteins mixture, especially from insoluble membrane fractions. For the complete glycosylation analysis, we examined the extraction of a whole glycoprotein from the gel, followed by trypsin digestion. Additionally, for the effective glycopeptide analysis, we studied mass spectrometric peptide/glycopeptide mapping by LC/MS^n with in-source CID and data-dependent MS^n. The glycopeptides were localized in the peptide/glycopeptide map by using oxonium ions as marker ions such as $HexNAc^+$ and $NeuAc^+$, which were generated by in-source CID, and neutral loss by data-dependent CID-MS/MS. For simultaneous identification of both peptides and glycopeptides, we conducted the database search analysis using search parameters containing a possible glycosylation at Asn with GlcNAc (203 Da). We successfully determined the sequences of peptides and some of the glycopeptides, which were localized by in-source CID and data-dependent CID-MS^n. The database search analysis using these search parameters was useful for identifying the glycopeptides resulting from predictable proteinase digestion. Glycopeptides caused by irregular digestion could be identified by assignment of peptide b and y series ions, which arose from further MS^n. The oligosaccharide structures of the identified glycopeptides were characterized on the basis of their product ion spectra. In this way, we were able to isolate rat brain Thy-1 and to elucidate *N*-glycosylation at Asn23, 74, and 98 as well as the structure of the GPIs at Cys111.

Post-translationally modified peptides could not be identified by the database search analysis. It has been particularly difficult to identify glycopeptides by database search analysis due to their complicated product ions resulting from the cleavage of glycosidic bonds. It has recently been reported that peptide + GlcNAc ion generated from a glycopeptide by CID-MS/MS yields b and y series ions by further MS^n, and that these ions can be utilized for identification of the peptide backbone and its glycosylation site [15,16,18]. Additionally, search analysis using the database including the possibility of glycosylation at Asn with all possible cleavage products of the known glycopeptides can be utilized for identification of glycopeptides in the peptide/glycopeptide map [19]. This ability would be helpful in the identification of glycoproteins whose glycosylation are already known. In the present study, we carried out a database search analysis using search parameters containing a possible glycosylation at Asn with only GlcNAc (203 Da), and successfully identified an unknown glycoprotein and *N*-glycosylated sites. This search analysis can be used for the identification of *O*-glycosylation, which has no consensus amino acid sequence, by using search parameters containing possible glycosylations at Ser/Thr with Hex, HexNAc, and dHex.

Precursor ion scans have been used for the localization the glycopeptides in peptide/glycopeptide mapping [10,11,13]. Although this method can be used for monitoring the peptides with predictable modification by setting mass of fragment ions prior to scanning, peptides with unpredictable modification cannot be detected. In contrast, in-source CID and CID-MS/MS are capable of localizing of the modified peptides after just one data acquisition using objective oxonium ions and neutral losses. In the present study, we were able to localize GPI-peptides in the peptide/glycopeptide map using EtN-PO_4-Man^+ and GlcN-Inositol-$PO_4{}^+$ generated by in-source CID [25] and to elucidate the GPI structures. We also could localize the glycopeptides with dHex, HexNAc, and NeuAc at the non-reducing ends as well as Hex using neutral loss by CID-MS/MS.

Site-specific glycosylation analysis of rat brain Thy-1 was performed after purification with monoclonal antibody affinity chromatography. Released oligosaccharides from fractionated trypsin-digested glycopeptides were analyzed by conventional analytical methods, including exoglycosidase digestion and methylation analysis [26]. In the present study, we separated PIPLC-treated GPI-anchored proteins of rat brain by SDS-PAGE, and conducted site-specific glycosylation analysis by LC/MS^n. Using a simpler step, we could elucidate the glycosylation at each glycosylation site with a greater variety of oligosaccharides than that reported previously and four GPI structures, including two novel attached structures.

Our strategy presented herein can relatively simply facilitate complete site-specific glycosylation analysis that used to require a series of complicated steps and is applicable to characterization of unknown proteins on 2-DE gel in proteomic study. Even in a mixture of multiple unknown glycoproteins, glycosylation of each glycoprotein can be determined based on the product ion spectra. Our method would be helpful for study of the alternation of glycosylation with growth, aging, and disease [27,28].

Acknowledgements

This study was supported in part by a Grant-in-Aid from the Ministry of Health, Labor and Welfare, Core Research for the Evolutional Science and Technology Program (CREST) of the Japan Science and Technology Agency (JST), and Research on Health Science focusing on Drug Innovation from The Japan Health Science Foundation (N.K.).

We appreciate Dr. A. Hachisuka of the National Institute of Health Science for her technical advice.

We would also like to thank Dr. M. Kubota and Mr. M. Yoshida of Thermo Electron K.K. (Japan), for their technical support.

References

[1] A. Varki, Glycobiology 3 (1993) 97.
[2] H. Sasaki, B. Bothner, A. Dell, M. Fukuda, J. Biol. Chem. 262 (1987) 12059.
[3] F. Wang, A. Nakouzi, R.H. Angeletti, A. Casadevall, Anal. Biochem. 314 (2003) 266.
[4] K. Hirayama, R. Yuji, N. Yamada, K. Kato, Y. Arata, I. Shimada, Anal. Chem. 70 (1998) 2718.
[5] M. Ohta, N. Kawasaki, S. Itoh, T. Hayakawa, Biologicals 30 (2002) 235.
[6] E. Mortz, T. Sareneva, S. Haebel, I. Julkunen, P. Roepstorff, Electrophoresis 17 (1996) 925.
[7] F.G. Hanisch, M. Jovanovic, J. Peter-Katalinic, Anal. Biochem. 290 (2001) 47.
[8] D. von Witzendorff, M. Ekhlasi-Hundrieser, Z. Dostalova, M. Resch, D. Rath, H.W. Michelmann, E. Topfer-Petersen, Glycobiology 15 (2005) 475.
[9] B. Küster, T.N. Krogh, E. Mortz, D.J. Harvey, Proteomics 1 (2001) 350.
[10] S.A. Carr, M.J. Huddleston, M.F. Bean, Protein Sci. 2 (1993) 183.
[11] M.J. Huddleston, M.F. Bean, S.A. Carr, Anal. Chem. 65 (1993) 877.
[12] R.S. Annan, S.A. Carr, J. Protein Chem. 16 (1997) 391.
[13] K. Sandra, I. Stals, P. Sandra, M. Claeyssens, J. Van Beeumen, B. Devreese, J. Chromatogr. A 1058 (2004) 263.
[14] A. Harazono, N. Kawasaki, T. Kawanishi, T. Hayakawa, Glycobiology 15 (2005) 447.
[15] U.M. Demelbauer, M. Zehl, A. Plematl, G. Allmaier, A. Rizzi, Rapid Commun. Mass Spectrom. 18 (2004) 1575.
[16] Y. Wada, M. Tajiri, S. Yoshida, Anal. Chem. 76 (2004) 6560.
[17] B. Sullivan, T.A. Addona, S.A. Carr, Anal. Chem. 76 (2004) 3112.
[18] S. Zhang, D. Chelius, J. Biomol. Tech. 15 (2004) 120.
[19] S. Wu, P. Bondarenko, T. Shaler, P. Shieh, W. Hancock, Thermo Finnigan LC/MS^n Application Report Application Report No. 300.
[20] C. Bordier, J. Biol. Chem. 256 (1981) 1604.
[21] M.P. Lisanti, M. Sargiacomo, L. Graeve, A.R. Saltiel, E. Rodriguez-Boulan, Proc. Natl. Acad. Sci. U.S.A. 85 (1988) 9557.
[22] S. Itoh, N. Kawasaki, M. Ohta, T. Hayakawa, J. Chromatogr. A 978 (2002) 141.
[23] B. Domon, C.E. Costello, J. Glycoconjugate 5 (1988) 397.
[24] S.W. Homans, M.A. Ferguson, R.A. Dwek, T.W. Rademacher, R. Anand, A.F. Williams, Nature 333 (1988) 269.
[25] K. Fukushima, Y. Ikehara, M. Kanai, N. Kochibe, M. Kuroki, K. Yamashita, J. Biol. Chem. 278 (2003) 36296.
[26] R.B. Parekh, A.G. Tse, R.A. Dwek, A.F. Williams, T.W. Rademacher, EMBO J. 6 (1987) 1233.
[27] Y. Sato, M. Kimura, C. Yasuda, Y. Nakano, M. Tomita, A. Kobata, T. Endo, Glycobiology 9 (1999) 655.
[28] G. Durand, N. Seta, Clin. Chem. 46 (2000) 795.